Obestatin regulates adipocyte function and protects against diet-induced insulin resistance and inflammation

Abstract

The metabolic actions of the ghrelin gene-derived peptide obestatin are still unclear. We investigated obestatin effects in vitro, on adipocyte function, and in vivo, on insulin resistance and inflammation in mice fed a high-fat diet (HFD). Obestatin effects on apoptosis, differentiation, lipolysis, and glucose uptake were determined in vitro in mouse 3T3-L1 and in human subcutaneous (hSC) and omental (hOM) adipocytes. In vivo, the influence of obestatin on glucose metabolism was assessed in mice fed an HFD for 8 wk. 3T3-L1, hSC, and hOM preadipocytes and adipocytes secreted obestatin and showed specific binding for the hormone. Obestatin prevented apoptosis in 3T3-L1 preadipocytes by increasing phosphoinositide 3-kinase (PI3K)/Akt and extracellular signal-regulated kinase (ERK)1/2 signaling. In both mice and human adipocytes, obestatin inhibited isoproterenol-induced lipolysis, promoted AMP-activated protein kinase phosphorylation, induced adiponectin, and reduced leptin secretion. Obestatin also enhanced glucose uptake in either the absence or presence of insulin, promoted GLUT4 translocation, and increased Akt phosphorylation and sirtuin 1 (SIRT1) protein expression. Inhibition of SIRT1 by small interfering RNA reduced obestatin-induced glucose uptake. In HFD-fed mice, obestatin reduced insulin resistance, increased insulin secretion from pancreatic islets, and reduced adipocyte apoptosis and inflammation in metabolic tissues. These results provide evidence of a novel role for obestatin in adipocyte function and glucose metabolism and suggest potential therapeutic perspectives in insulin resistance and metabolic dysfunctions.

_____

White adipose tissue (WAT) plays a key role in energy homeostasis and endocrine functions by secreting different hormones and adipokines influencing pathophysiological processes such as growth and differentiation, glucose homeostasis, and cancer (1). Increased WAT mass, as in obesity, is accompanied by chronic systemic inflammation, characterized by increased macrophage infiltration in WAT and elevated production of proinflammatory cytokines, both activating inflammatory pathways in adipocytes. The consequent changes in secretion of WAT-derived factors contribute to the development of obesity-associated pathologies like insulin resistance and type 2 diabetes (T2D; refs. 2, 3).

Obestatin is a 23-aa amidated peptide encoded by the ghrelin gene and mainly produced by the stomach. Obestatin was found to interact with the orphan receptor G-protein-coupled receptor 39 (GPR39) and to oppose the stimulatory effect of acylated ghrelin (AG) on food intake and gastrointestinal motility (4,–,6). However, different studies failed to confirm obestatin anorexigenic effects, as well as GPR39 binding capacity (7,–,9), and obestatin biological actions are still debated.

Obestatin exerts both central and peripheral actions, including stimulation of cell survival and inhibition of apoptosis (10,–,12). Like AG and unacylated ghrelin (UAG), obestatin is mainly produced in the stomach, and at lower levels in the endocrine pancreas and different peripheral tissues (13,–,15). We have recently shown that obestatin exerts survival and antiapoptotic actions in pancreatic β cells and human pancreatic islets, regulates glucose-induced insulin secretion, and increases expression of key pancreatic genes (11). We have also suggested that obestatin may bind to the glucagon-like peptide 1 receptor (GLP-1R), which in turn would at least partly mediate the survival effects of the peptide in pancreatic β cells (11). Moreover, like ghrelin, obestatin prevents diabetes in streptozotocin-treated rats by improving glucose homeostasis and insulin secretion and increasing β-cell mass (16). Collectively, these findings strongly suggested a relevant metabolic role of the peptide.

Concerning WAT, although obestatin binding to GPR39 remains highly debated, GPR39 mRNA expression has been shown in different tissues, including human WAT (6, 17, 18). Moreover, Zhang et al. (6) reported Ob binding to recombinant GPR39 and to different tissues and GPR39-expressing cells, including WAT. Recently, obestatin effects in adipocyte metabolism and differentiation have been shown in 3T3-L1 adipocytes and rat adipose tissue (19, 20). However, knowledge on obestatin metabolic actions and its precise role in this context is still fragmentary and inconclusive and remains to be fully elucidated, particularly in primary human and mice adipocytes, as well as in whole metabolic function in an in vivo animal model. To circumvent this, we investigated the obestatin effects on adipocyte function in vitro, in both mice and human adipocytes, and examined its role on glucose metabolism and inflammation in vivo in mice fed a high-fat diet (HFD).

MATERIALS AND METHODS

Reagents

Human and mouse obestatin, mouse AG, and UAG were from Phoenix Pharmaceuticals (Karlsruhe, Germany). Insulin-like growth factor-I (IGF-I), human insulin, PD-98059, wortmannin, Hoechst-33258, isoproterenol (ISO), dexamethasone, 3-isobutyl-1-methylxanthine (IBMX), type 2 collagenase, bovine albumine, pantothenic acid, transferrin, biotin, 2-deoxi-d-glucose, Oil Red O, NH4CI, KHCO3, EDTA, and mammalian cell lysis kit were from Sigma-Aldrich (Milan, Italy). [3H]-2-deoxy-d-glucose was from Perkin Elmer Life Sciences (Boston, MA, USA). Cell culture reagents and AlexaFluor-labeled antibodies were from Invitrogen (Milan, Italy). P-Akt (Ser473) and P-extracellular signal-regulated kinase (ERK) antibodies were from Cell Signaling Technology (Celbio, Milan, Italy). ERK1/2, Akt, and GLP-1R antibodies were from Santa Cruz Biotechnology (DBA, Milan, Italy). Antibodies against P-AMP-activated protein kinase (P-AMPK; recognizing both α1 and α2 P-AMPK on T172), AMPK, sirtuin 1 (SIRT1), β-actin, glucose transporter type 4 (GLUT4), and GPR39 were from Abcam (Cambridge, UK). Horseradish peroxidase-conjugated secondary antibodies were from Bethyl Laboratories (Tema Ricerca, Bologna, Italy). ECL reagent was from Perkin Elmer Life Sciences. RT-PCR reagents were from PE Applied Biosystems (Milan, Italy).

Isolation and differentiation of human adipocytes

Subcutaneous (SC) and omental (OM) fat tissue was obtained during laparoscopic surgery for nonmalignant diseases from 35 obese nondiabetic and 6 lean adult subjects, who had given informed consent before surgery. The study protocol was approved by the local ethics committee (Department of Internal Medicine, University of Turin). Adipocyte isolation was performed as described previously (21). At confluence,

preadipocyte culture medium was changed to DMEM (Life Technologies; Invitrogen) containing 10% FBS, 15 mM HEPES, 33 μM biotin, 17 μM pantothenate, 10 μg/ml transferrin, 5 μg/ml human insulin, 1 μM dexamethasone, and 0.5 mM IBMX for 3 d to initiate differentiation. At d 4, dexamethasone and IBMX were removed from the medium; cells were refed every 3 d and harvested at d 0, 7, 14, and 21 of differentiation. Preadipocytes maintained in DMEM/F12 supplemented with 10% FBS were used as controls.

3T3-L1 cell culture

3T3-L1 preadipocytes (ATCC, Manassas, VA, USA) were maintained in DMEM supplemented with 10% FCS. At 2 d after confluence (d 0), cells were treated with differentiation medium (DM; 5 μg/ml insulin, 1 μM dexamethasone, and 0.5 mM IBMX) in DMEM supplemented with 10% FBS. At 2 d after treatment, cells were maintained in DMEM supplemented with 10% FBS and 1 μg/ml insulin for up to 8 d, with a medium change every 2 d. 3T3-L1 differentiation was monitored by visualizing lipid droplets under light microscopy stained with 5% Oil Red O in 60% ISO.

Imaging and flow cytometric analysis of obestatin binding and expression

3T3-L1 and human preadipocytes were grown on coverslips up to 50–60% confluence. A labeled obestatin derivative, TAMRA-obestatin (Inbios, Naples, Italy), was used to visualize obestatin binding sites. TAMRA-obestatin specificity toward obestatin binding sites was tested in competition experiments. Obestatin binding on 3T3-L1 preadipocytes and adipocytes (d 8) was assessed by exposing the cells to 1.5 μM TAMRA-obestatin in serum-free DMEM at 37°C for 20 min after 10 min of preincubation at 4°C, when unlabeled obestatin (from 10 nM to 2 μM) or unrelated competitors (1 μM) were added. Cells were subsequently washed in PBS, fixed in 3% paraformaldehyde, and processed for microscopy. TAMRA-obestatin-specific binding to human subcutaneous (hSC) preadipocytes was tested as described for 3T3-L1. Confocal microscopy analysis was performed using a Zeiss LSM 5 Pascal Model Confocal Microscope (Carl Zeiss International, Oberkochen, Germany). For flow cytometric analysis, cells were analyzed using a FACSCanto and Diva software (Beckton Dickinson, Franklin Lakes, NJ, USA). Ten thousand events were analyzed for each sample. Obestatin protein expression was determined by immunofluorescence in normal hSC and human omental (hOM) tissue, both obtained from surgical specimens of patients who underwent surgery for nontumoral diseases. Tissues were fixed and stained using a rabbit obestatin polyclonal antibody (diluted 1:300; Phoenix Pharmaceuticals), followed by FITC-conjugated goat anti-rabbit antibody (diluted 1:200; Abcam).

RT-PCR and real-time PCR

Total RNA extraction from 3T3-L1, hSC, and hOM adipocytes and reversed transcription to cDNA from 3 μg RNA were performed as described previously (22). RT-PCR primers were synthesized by TibMol Biol (Genoa, Italy) and Tema Ricerca (Bologna, Italy). The following primer sequences were used: mouse GPR39, Fwd 5′-CCCTATAACACAGGCCCAGA-3′ and Rev 5′-CACCCAAAAGAACTCCCAGA-3′ (accession no. BC_085285); human GPR39, Fwd 5′-AGGTGCTGCAGAAGAAAGGA-3′ and Rev 5′-GCCTCGAAGAGGAAAGTGTG-3′ (accession no. NM_001508); 18S rRNA, Fwd 5′-GTGGAGCGATTTGTCTGGTT-3′ and Rev 5′-CGCTGAGCCAGTTCAGTGTA-3′ (accession no. X_01117); mouse SIRT1, Fwd 5′-GCTCGCCTTGCGGTGGACTT-3′ and Rev 5′-TGGCTCATCAGCTGGGCACC-3′ (accession no. NM_019812.2). cDNA (9 μl) was amplified (GeneAmp PCR System; Perkin Elmer, Milan, Italy) in 50 μl under the following conditions: 94°C for 30 s, for 64°C for 30 s annealing; 72°C for 30 s, 72°C for 7 min. The final PCR products were separated by 1.5% agarose gel electrophoresis and visualized by ethidium bromide staining. For real-time PCR, the following primers were used: preproghrelin, Fwd 5′-CTGCTGATACTGAGCTCCTGACAG-3′ and Rev 5′-

AGGAGCTGGAGAGATCAGGTTCAAT-3′ (accession no. NM_021488.4); 18s rRNA, Fwd 5′-CCCATTCGAACGTCTGCCCTATC-3′ and Rev 5′-TGCTGCCTTCCTTGGATGTGGTA-3′ (accession no. NR_003278.3). Real-time PCR was performed with 50 ng of cDNA, 150 nM of each primers, and a 2× Master Mix (annealing 61°C) using ABI-Prism 7300 (Applied Biosystems).

GLUT4 immunofluorescence

3T3-L1 cells were grown on glass coverslips and differentiated. On d 8, they were serum starved for 2 h at 37°C and treated with either 100 nM insulin or 10 nM or 100 nM obestatin for 30 min and then washed twice with 1× PBS. The cells were then fixed with 4% paraphormaldeyde, permeabilized, and incubated with anti-GLUT-4 antibody. After being washed 3 times with 1× PBS, cells were incubated with AlexaFluor 488-conjugated goat anti-mouse IgG (Invitrogen) for 1 h at room temperature. Cytoplasmic and surface-membrane-bound GLUT-4 were visualized using confocal laser scanning microscopy (Leica TCS SP2). Nuclei were stained with DAPI. Fluorescence excitation was obtained at 488 nm via argon/krypton laser line for Alexa 488. DAPI was detected by Coherent Enterprise II 351/364-nm laser lines (Coherent Inc., Santa Clara, CA, USA). Green and blue channels were assigned to GLUT-4 and the nuclei, respectively. Single-labeled and negative (i.e., isotype-matched) controls were also analyzed. Cytoplasmic and surface-membrane-bound GLUT-4 were visualized using confocal laser scanning microscopy (Leica TCS SP2).

Cell proliferation and survival

3T3-L1 preadipocyte cell proliferation was assessed by bromodeoxyuridine incorporation ELISA (Roche, Indianapolis, IN, USA), as described previously (11). Cell survival was assessed by trypan blue exclusion on 3T3-L1 preadipocytes. Cells were stained with trypan blue dye (0.04% w/v; Invitrogen). Viable (unstained) and nonviable (blue-stained) cells (300 cells/dish) were counted with a Countess automated cell counter (Invitrogen).

Hoechst staining and caspase 3 activity

Morphological changes in the nuclei of apoptotic preadipocytes were detected by Hoechst 33258, as described previously (11). Caspase 3 activity was assessed by caspase-3 colorimetric kit (Assay Designs, Milan, Italy) in preadipocyte cell lysates, according to the manufacturer's instruction.

Western blotting

Immunoblot analysis were performed as described previously (11). Proteins were extracted from 3T3-L1 and human adipocytes and from mouse soleus muscle, adipose tissue, and liver. Proteins (50 μg) were resolved in 10% SDS-PAGE and incubated with the specific antibody (P-ERK1/2, P-AKT, P-AMPK, SIRT1, and GLP-1R). Blots were reprobed with the respective total antibodies against or β-actin (for SIRT1 and GLP-1R) for normalization. Immunoreactive proteins were visualized with Chemidoc XRS (Bio-Rad, Milan Italy), and densitometric analysis was performed with Quantity One software (Bio-Rad).

Protein secretion from adipocytes

Obestatin secretion was assessed in concentrated (18-fold) culture medium from differentiating adipocytes (3T3-L1, hSC, and hOM) using the obestatin radioimmunoassay (RIA) kit (Phoenix Pharmaceuticals), following the manufacturer's instruction. Obestatin in cell culture medium (50 μl DMEM+10% FBS), either in the presence or absence of 3T3-L1 preadipocytes or adipocytes, was measured using the obestatin (rat and mouse) enzyme immunoassay (EIA) kit (EK-031-90; Phoenix Pharmaceuticals), following the

manufacturer's instructions. Adiponectin and leptin secretion was evaluated in hSC adipocyte concentrated (18-fold) conditioned medium using the human and mouse adiponectin ELISA kit and the human leptin ELISA kit, respectively (R&D Systems, Minneapolis, MN, USA), following the manufacturer's instructions. tumor necrosis factor α (TNF-α) and interleukin-1β (IL1-β) were measured by specific ELISA kits (eBioscience, San Diego, CA, USA) and adiponectin quantified with the human and mouse adiponectin ELISA (R&D Systems). Briefly, mouse tissues (epididymal and SC adipose tissue, soleus muscle, and liver) were cut into small pieces and lysed with mammalian cell lysis kit (Sigma-Aldrich). Monoclonal antibodies specific for each cytokine were precoated onto microplates. Samples were then pipetted into the wells, and any cytokine present was bound by the immobilized antibody. After any unbound substances were washed away, an enzyme-linked polyclonal antibody specific for each cytokine was added to the wells. Following another wash, a substrate solution was added to the wells, the enzyme reaction was stopped with the addition of a stop solution, and the samples were quantified with a microplate reader.

Triglyceride (TG) measurement

TG content was determined using a colorimetric assay kit (Zen-Bio, Research Triangle Park, NC, USA) and normalized against total protein from each sample, determined by Bradford reagent (Sigma).

Lipolysis assay

Forty microliters of the floating fraction containing only differentiated adipocytes (for both 3T3-L1 and human adipocytes) was seeded into a 96-well plate, containing 100 µl of lipolysis assay kit buffer (Zen-Bio) in the presence or absence of either obestatin (1, 10 and 100 nM) or insulin (100 nM), as described previously (23). After 40 min, ISO (1 µM) was added to the wells, and incubation was carried out for a further 80 min. Following the manufacturer's instructions, 50 µl of medium was then transferred into a new 96-well plate for glycerol measurement on a microplate reader at 570 nm (Eti System Fast Reader ELX; BioTek Instruments, Winooski, VT, USA). The amount of glycerol release was calculated as micromoles per milligram of protein and expressed as percentage of ISO-induced lipolysis.

[3H]-2-deoxyglucose uptake

Differentiated 3T3-L1 (d 8) and hSC adipocytes (d 21) were serum starved overnight at 37°C and then incubated with obestatin (10 or 100 nM), either with or without insulin (100 nM) for 20 min. Cells were then rinsed with glucose-free HEPES-buffered saline solution (140 mM NaCl, 20 mM HEPES/Na, 5 mM KCl, 2.5 mM MgSO4, and 1 mM CaCl2 at pH 7.4) and incubated in the same buffer at 37°C for 10 min with 2 mM 2-deoxyglucose containing 0.1 µCi/ml [3H]-2-deoxyglucose. Under these conditions, glucose uptake was linear for ≥20 min (data not shown). Uptake was stopped by rapid removal of the buffer, followed by 3 washes in ice-cold PBS. Cells were solubilized by addition of 50 mM NaOH, and equal amounts of lysates were subjected to liquid scintillation counting (Beckman Instruments, Fullerton, CA, USA) to measure, in duplicate, cell radioactivity. Protein concentrations were determined using the BCA kit (Sigma-Aldrich). Uptake values, expressed as picomoles per minute of [3H]-2-deoxyglucose incorporated per milligrams of protein, were corrected for the non-carrier-mediated transport by measuring hexose uptake in the presence of 10 µM cytochalasin B (a potent inhibitor of facilitated glucose transport). The nonspecific association of deoxyglucose with the cells was typically <10% of the total uptake.

Small interfering RNA (siRNA)

siRNAs targeting mouse SIRT1 and GLP1-R mRNA were synthesized by Qiagen (Milan, Italy) using the SIRT1 target sequence: 5′-CAGATTGTTATTAATATCCTT-3′, sense: 5′-GAUUGUUAUUAAUAUCCUUTT-3′, antisense:

5′-AAGGAUAUUAAUAACAAUCTG-3′; GLP-1R target sequence: 5′-TAGGAACTCCAATATGAACTA-3′, sense: 5′-GGAACUCCAAUAUGAACUATT-3′, antisense: 5′-UAGUUCAUAUUGGAGUUCCTA-3′; and the control nonsilencing siRNA (catalog no. 1022076). 3T3-L1 preadipocytes (2 d postseeding) and differentiated adipocytes (d 7) were transfected in Opti-MEM I reduced serum medium without antibiotics with 50 nM control, SIRT1, or GLP-1R siRNAs using Lipofectamine RNAiMAX (Invitrogen) as recommended by the manufacturer. The medium was replaced with normal growth medium containing insulin after 4 h. Cells were transfected again after 48 h for glucose uptake experiments. Efficiency of transfection was assessed by RT-PCR and Western blot.

Animals

Mouse procedures conformed to the U.S. National Institutes of Health Guide for Care and Use of Laboratory Animals, and all procedures were approved by the Animal Care and Use Committee of the University of Turin. Male C57BL6/J (7-wk-old) mice were purchased from Charles River Laboratories (Lecco, Italy) and maintained with a standard diet and tap water ad libitum for 1 wk. Then, mice were separated into 4 groups (n=14/group): mice fed a low-fat diet (LFD; 10% energy as fat) and intraperitoneally injected for 1 wk with either saline (group 1) or obestatin (group 2; 1 μmol/kg/d); or fed an HFD (60% energy as fat) and similarly injected with saline (group III) or obestatin (group IV) for 1 wk. LFD and HFD were formulated by Mucedola Srl (Settimo Milanese, Italy). Injections were repeated for 3 d at d 25 and at d 39. Animals were weighed 1×/wk and after 8 wk (56 d) were anesthetized with tribromoethyl alcohol (Avertin; 375 mg/kg i.p.). Blood samples were collected from the heart, and plasma glucose levels were determined using a glucose analyzer. Blood was then centrifuged at 20,000 g for 2 min at 4°C and stored at ∼20°C until use. Pancreas, liver, muscle, epididymal, and SC adipose tissue were rapidly excised and weighed. Tissues were either frozen in liquid nitrogen or homogenized in 4 M guanidine isothiocyanate buffer or fixed in neutral buffered formalin for protein analysis or total RNA extraction or histological examination, respectively. Plasma and pancreatic insulin were assessed as described previously (16) using an RIA kit (DiaSorin, Saluggia, Italy) or an ELISA kit (Millipore, Bedford, MA, USA) (24). Plasma obestatin was measured using the obestatin (rat, mouse) EIA kit (EK-031-90; Phoenix Pharmaceuticals), following the manufacturer's instructions. TNF-α and IL1-β were measured by specific ELISA kits (eBioscience), and adiponectin was quantified with the human and mouse adiponectin ELISA (R&D Systems), following the manufacturer's instruction. Caspase-3 activity was assessed by caspase-3 colorimetric kit (Assay Designs) in adipose cell lysates, as previously reported (11). In a second group of mice (n=5–10 mice/group), a glucose tolerance test (GTT; glucose 1 g/kg i.p.; overnight unfed condition) and insulin tolerance test (ITT; insulin 0.75 U/kg; fed condition) were performed in LFD- and HFD-fed control and obestatin-treated mice, as previously reported (24). Glucose levels were assessed by Glucocard G glucometer (Arkray, Kyoto, Japan) before injection (t0) and 15, 30, 60, and 120 min after injection of glucose or insulin. Circulating insulin levels, assessed by ELISA (Millipore) were compared between LFD- and HFD-fed control and obestatin-treated mice at t0 and t30 of the GTT. Circulating obestatin levels were measured with the mouse ELISA kit (Phoenix pharmaceuticals). Food intake was measured daily during the week before euthanasia, and energy intake was calculated based on diet composition. Morphometric analysis was performed using a digital microscope (DMD108; Leica MicroSystems) and included the evaluation of the mean islet area (evaluated in up to 10 islets for each case) and the number of epididymal or SC adipocytes, calculated as the mean number of adipocytes counted in 3 randomly selected fields viewed at ×400.

Quantification of pancreatic insulin content

Pancreas was homogenized and centrifuged in 5 ml acid-ethanol [0.15 M HCl in 75% (v/v) ethanol] at 1000 g for 20 min; the supernatants were stored at −80°C, and the insulin was then quantified by RIA (DiaSorin) and normalized to milligrams of total protein (25).

Quantification of insulin release from mouse pancreatic islets

Glucose-stimulated insulin release from mouse pancreatic islets was assessed as described previously (26). Briefly, freshly removed pancreas was trimmed of adherent fat and connective tissue and minced into pieces of ∼40 mg. The pieces were washed in 15 ml polypropylene tubes containing 1 ml of Krebs buffer to dilute digestive hormones and preincubated for 30 min at 37°C. The buffer was then carefully drained, and the specimens were further incubated 1 h in either the absence or presence of different concentrations of glucose (2.8, 8.3, and 16.7 mM). The tissues were then pelleted, and the supernatants were collected and stored at −80°C. Insulin release in the supernatant was quantified by RIA (DiaSorin) and normalized to milligrams of total protein.

Isolation of mouse adipocytes

After excision, 500 mg of SC or eipididymal adipose tissue was cut into small pieces and digested at 37°C for 2 h in DMEM with 1 mg/ml of type 2 collagenase (Sigma-Aldrich). Mature adipocytes were isolated as described previously (21).

Glucose uptake in mouse WAT explants

[3H]-2-deoxyglucose uptake in mouse epididymal adipose tissue was determined immediately after death, as described previously (27, 28). Adipose tissue (50 mg) was preincubated for 10 min at 37°C in 1 ml of Krebs-Ringer-HEPES (KRH) buffer (50 mM HEPES, pH 7.4; 137 mM NaCl; 4.8 mM KCl; 1.85 mM CaCl2; and 1.3 mM MgSO4), also used for subsequent incubations. Incubation with or without 100 nM insulin was carried out at 37°C for 10 min. A stop solution and 2 washes in ice-cold KRH buffer were used to remove unbound [3H]-2-deoxyglucose and to block glucose transport. To facilitate measurement of the incorporated radioactive deoxyglucose, tissues were further dissolved in collagenase (1 mg/ml; Sigma-Aldrich) at 37°C for 20 min and homogenized by tissue lyser (120 V, 50/60 Hz, 5 min; Qiagen). Data were expressed as picomoles per minute of [3H]-2-deoxyglucose incorporated per milligrams of tissue (wet weight). Nonspecific binding was determined under the same conditions in the presence of 50 µM cytocalasin B.

Lipolysis assay in mouse WAT explants

Mouse epididymal adipose tissue was cut into small pieces (300 mg), transferred into 15-ml tubes, and digested at 37°C for 2 h in DMEM with 1 mg/ml type 2 collagenase (Sigma-Aldrich). After the first centrifugation, the mature adipocytes formed a floating ring that was then collected and transferred into 2-ml tubes. After additional washing and centrifugation steps, 40 µl of the floating fraction containing only mature adipocytes was seeded into a 96-well plate containing 100 µl of lipolysis assay kit buffer (Zen-Bio). Following the manufacturer's instructions, 50 µl of medium was transferred into a new 96-well plate, and the detection of glycerol amount was assessed by spectrophotometry at 570 nm absorbance using a 96-well plate reader (Eti System Fast Reader ELX), calculated as micromoles per milligram of protein and expressed as a percentage of ISO-induced lipolysis.

Statistical analysis

Results are presented as means ± se. Calculations were performed using GraphPad Prism 5.0 software (GraphPad Software, San Diego, CA, USA). Statistical analyses were performed with Student's t test for independent samples or by 2-way ANOVA followed by Newman-Keuls post hoc test for multiple group comparisons. Significance was established as a value of $P < 0.05$.

RESULTS

Obestatin binds to and is secreted from 3T3-L1 cells and human adipocytes

Confocal microscopy analysis in either the presence or absence of fluorescent TAMRA-obestatin was performed to investigate obestatin binding to 3T3-L1 and hSC preadipocytes, maintained 2 d in DM. Binding of TAMRA-obestatin was evidenced in both 3T3-L1 and hSC preadipocytes and was displaced in a dose-dependent manner by unlabeled obestatin (10 nM to 2 μM), but not by BIM23627, a type 2 somatostatin receptor antagonist used as negative control (Fig. 1A, B). Complete displacement by unlabeled obestatin at concentrations equal or higher than 100 nM demonstrated high affinity of TAMRA-obestatin for obestatin-binding sites (Fig. 1A, B). Human SC preadipocytes maintained in non-DM showed obestatin-binding capacity (Supplemental Fig. S1A). We previously showed partial obestatin binding to the GLP-1R in pancreatic β cells (11). Here, TAMRA-obestatin was displaced by the GLP-1R agonist exendin-4 (Ex-4) and by the antagonist exendin-9 (Ex-9) in both 3T3-L1 and hSC adipocytes (Fig. 1A, B). These results suggested specific obestatin interaction with GLP-1R in adipocytes. In further support of this assumption, obestatin binding in 3T3-L1 preadipocytes was prevented by siRNA against GLP-1R (Fig. 1A), which reduced GLP-1R protein expression by ∼40% (Fig. 1C) but not by control siRNA. Similar results were obtained in differentiated 3T3-L1 adipocytes (Supplemental Fig. S1C, D).

Figure 1.

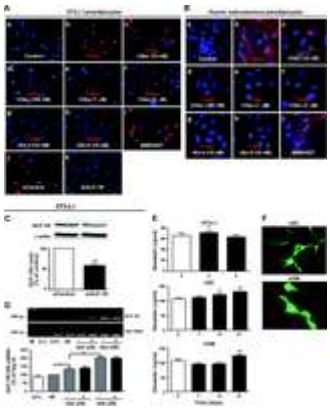

Figure 1.

Obestatin binding and secretion in 3T3-L1 and human preadipocytes. A) a–h) Confocal microscopy analysis of 3T3-L1 cells incubated for 48 h in DM in either the absence (control; a) or presence of TAMRA-obestatin (T-obe; 1.5 μM; b–h). Binding of TAMRA-obestatin is shown in red, and nuclei are stained in blue (DAPI). c–f) Displacement of TAMRA-obestatin with increasing concentrations of unlabeled obestatin: 10 nM (c), 100 nM (d), 1 μM (e), 2 μM (f). g, h) Displacement of TAMRA-obestatin binding with Ex-4 (g) or Ex-9 (h). i) BIM23627 was used as negative control for TAMRA-obestatin displacement. j, k) Inhibition of TAMRA-obestatin binding by siGLP1-R (k) but not by

siControl (j). View: ×40. B) a–i) Confocal microscopy analysis of hSC preadipocytes incubated in either absence (control; a) or presence of 1.5 μM TAMRA-obestatin (b–i). c–f) Displacement of TAMRA-obestatin binding with increasing concentrations of unlabeled obestatin: 10 nM (c), 100 nM (d), 1 μM (e), 2 μM (f). g, h) Displacement of TAMRA-obestatin binding with Ex-4 (g) or Ex-9 (h). i) BIM23627 (1 μM) was used as negative control. View: ×100. C) GLP-1R protein expression, assessed by Western blot in 3T3-L1 preadipocytes after 48 h transfection with either siControl or siGLP-1R. Blots were reprobed with anti-β-actin antibody. Graphs represent the densitometric analysis of GLP-1R normalized to β-actin and reported as percentage of siControl (n=3). Data are means ± se of 3 independent experiments. **P < 0.01. D) GLP-1R mRNA, assessed by RT-PCR in 3T3-L1 adipocytes at the indicated days of differentiation, in the absence or presence of obestatin (10 nM). Results normalized to 18S rRNA transcript are expressed as percentage of control (d 0; n=3). Data are means ± se of 3 independent experiments. *P < 0.05, **P < 0.01. E) Obestatin secretion from 3T3-L1, hSC, and hOM adipocytes at the indicated days of differentiation. *P<0.05; **P<0.01 vs. d 0. F) Obestatin protein expression in hSC and hOM adipocytes, assessed by fluorescence microscopy (×100 view; n=3).

GLP-1R mRNA expression was determined during differentiation of 3T3-L1 adipocytes that were either untreated or treated with obestatin. GLP-1R mRNA in untreated cells increased at d 4 as compared with d 0 and was further up-regulated at the end of differentiation (d 8). Obestatin did not influence GLP-1R expression at any day of differentiation (Fig. 1D).

Flow cytometry analysis indicated that in 3T3-L1 preadipocytes, both the mean fluorescent index and the percentage of ligand-bound fluorescent cells increased with 1.5 μM and even more with 2 μM TAMRA-obestatin. In hSC preadipocytes, TAMRA-obestatin binding peaked at 1.5 μM and decreased at 2 μM, suggesting saturation of obestatin binding sites (Supplemental Fig. S1B).

Obestatin secretion in preadipocyte culture medium (d 0) increased at d 4 of differentiation in 3T3-L1 cells, at d 14 and 21 in hSC, and at d 21 in hOM adipocytes (Fig. 1E). Obestatin was not detected in cell-free DM, indicating exclusive production by adipocytes (data not shown). Obestatin in human adipocytes was further demonstrated by immunofluorescence staining, showing diffused cytoplasmic distribution (Fig. 1F).

Obestatin prevents apoptosis of 3T3-L1 preadipocytes through phosphoinositide 3-kinase (PI3K)/Akt and ERK1/2 signaling

Based on the previously observed antiapoptotic actions (11), we appraised the potential obestatin inhibitory effects against serum starvation-induced apoptosis in 3T3-L1 preadipocytes. Apoptosis increased under serum deprivation and was inhibited by IGF-I, which was used as control peptide (Fig. 2A, B). Similarly, IGF-I increased cell survival, which was strongly reduced by serum starvation (Fig. 2C). Obestatin had no effect at the lower concentrations tested (1 and 10 pM), whereas it reduced the percentage of

apoptotic nuclei at the highest concentrations (100 pM to 100 nM; Fig. 2A). Moreover, obestatin reduced caspase-3 activity at all the concentrations tested in the nanomolar range (Fig. 2B) and increased cell survival (Fig. 2C). These effects were equal to or even stronger than those of IGF-I, particularly at 10 and 100 nM. Peptide 14-1, the inverse sequence of UAG fragment 1-14, used as negative control, showed no survival or antiapoptotic effect.

Figure 2.

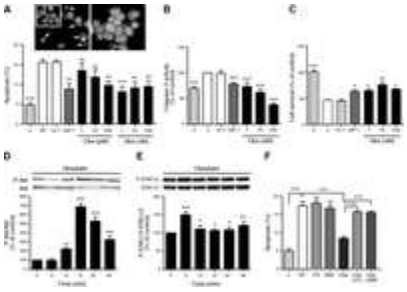

Figure 2.

Obestatin antiapoptotic effects in 3T3-L1 preadipocytes. A–C) Cells were cultured in the presence of serum (s) or in serum-free medium (SF) for 48 h, either with or without obestatin (Obe), at the indicated concentrations, peptide 14-1 (10 nM) or IGF-I (10 nM). A) Apoptosis measured by counting fragmented/condensed Hoechst-stained nuclei. Values are expressed as percentage of apoptotic cells obtained from duplicate determinations (500 cells each, n=3). Top panel: Hoechst 33258 nuclear immunofluorescence staining (×200). Obestatin was used at 10 nM. Inset: cells cultured with serum; arrows, apoptotic cells. B) Caspase-3 activity, expressed as percentage of control (c, SF; n=3). C) Cell survival assessed by trypan blue assay. Data, expressed as percentage of control (c, SF), are from 8 replicates (n=3). D, E) Akt (D) and ERK1/2 (E) phosphorylation, assessed by Western blotting on lysates from 3T3-L1 preadipocytes stimulated with 10 nM obestatin for the indicated times in SF medium (top panels). Equal protein loading was determined by reprobing with antibodies to the respective total proteins (bottom panels). Graphs represent the densitometric analysis of phosphorylated proteins normalized to total proteins and reported as percentage of basal (n=3). F) Apoptosis, assessed by Hoechst staining (48 h) in SF medium in the presence or absence of 10 nM obestatin and either PD98059 (40 μM) or wortmannin (WM; 100 nM). *P < 0.05, **P < 0.01, ***P < 0.001 vs. SF (A) control (B, C), or basal (D, E).

Next, we determined the involvement of the survival pathways PI3K/Akt and ERK1/2 in obestatin antiapoptotic effects. Based on the previous results, 10 nM was chosen as the best concentration for these experiments. Obestatin increased Akt phosphorylation at 10 min, peaking at 15 min and declining thereafter (Fig. 2D). ERK1/2 phosphorylation peaked at 5 min and then decreased, although it was up-regulated for up to 60 min (Fig. 2E). Obestatin antiapoptotic action was reduced by PD98059 and wortmannin, the specific ERK1/2 and PI3K/Akt inhibitors, respectively (Fig. 2F).

Obestatin effects on adipocyte differentiation

3T3-L1 preadipocytes were incubated with either control medium or DM in the absence or presence of obestatin for up to 8 d. At d 4, and particularly at d 8, lipid accumulation and size and number of lipid droplets increased in DM with respect to control medium, as determined by enhanced TG content and Oil Red O staining, respectively. Obestatin significantly increased lipid content in DM at d 8 but not at d 4 or in control medium (Fig. 3A).

Figure 3.

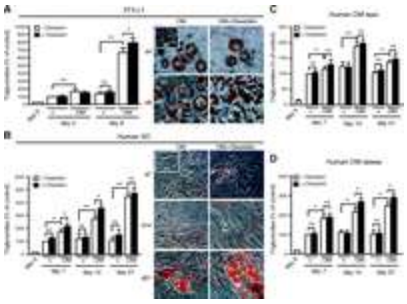

Figure 3.

Obestatin effects on adipogenesis of 3T3-L1 and human adipocytes. A) Two-day postconfluent 3T3-L1 preadipocytes were incubated for up to 8 d with either control medium or DM for induction of adipogenesis in either the absence or presence of obestatin (10 nM; d 0, cells in DM medium). TG content was measured at the indicated days using a colorimetric assay kit, as described in Materials and Methods, and expressed as percentage of control, d 4 (−obestatin). Right panel: representative Oil Red O staining of 3T3-L1 cells at the indicated days of differentiation in the absence or presence of obestatin (10 nM; ×40). B) hSC preadipocytes were grown to confluence and then treated without (c) or with DM for the indicated days for up to 21 d in either the absence or presence of obestatin (10 nM). TG content is expressed as percentage of control, d 7 (−obestatin). Right panel: Oil Red O staining of hSC at different days of differentiation either with or without obestatin (10 nM; ×40). C, D) TG content in human OM adipocytes obtained from lean (C) or obese (D) nondiabetic individuals. OM preadipocytes were grown to confluence and then treated as for hSC (B). Results are expressed as percentage of control, d 7 (−obestatin) and are means ± se of values obtained from cells cultured from 6 different individuals. *$P < 0.05$, **$P < 0.01$; ns, not significant.

Similarly, undifferentiated hSC adipocytes (d 0) had minimal TG stores and lipid droplets, which progressively increased up to d 21. Obestatin increased lipid content at d 7 and 14 in DM but not at d 21; no effect was observed in nondifferentiating control medium (Fig. 3B).

The obestatin adipogenic effect was also determined in hOM adipocytes obtained from both lean and obese individuals. As for hSC, hOM preadipocytes were cultured in DM for up to 21 d. In OM cells from lean individuals, obestatin showed no effect at any of the days examined (Fig. 3C). Conversely, in those from obese individuals, obestatin increased TG content at both d 14 and 21 in DM (Fig. 3D). No effect was observed in control medium from hOM cells derived from either lean or obese individuals.

Obestatin inhibits lipolysis in 3T3-L1 and human adipocytes

To assess the lipolytic effects of obestatin, differentiated 3T3-L1 cells and hSC and hOM adipocytes were treated either without or with ISO in the absence or presence of obestatin or insulin that was used as antilipolytic control peptide. Lipolysis was measured by the content of glycerol released in the culture medium. As expected, ISO increased lipolysis in both 3T3-L1 and human adipocytes, whereas insulin reduced lipolysis in both basal and ISO-stimulated conditions (Fig. 4A, D). In 3T3-L1 cells, obestatin had no effect on basal lipolysis; however, it reduced ISO-induced glycerol release, at both 10 and particularly 100 nM, but not at 1 nM (Fig. 4A). Similarly, in hSC cells, obestatin inhibited ISO-induced lipolysis at both 10 and 100 nM to a similar extent, whereas no effect was observed with 1 nM. In addition, at 100 nM, obestatin decreased basal glycerol release (Fig. 4B). In hOM adipocytes, obestatin showed similar antilipolytic effects at all concentrations tested in fat cells from both lean and obese individuals. In OM adipocytes from obese individuals, obestatin even inhibited basal lipolysis (at 10 and 100 nM; Fig. 4C, D). To determine whether the other products of the ghrelin gene, AG, and UAG would influence obestatin antilipolytic action, 3T3-L1 adipocytes were coincubated with obestatin and with AG, UAG, or the 2 peptides together. Neither AG nor UAG, nor a combination of both, showed any effect on the antilipolytic effect of obestatin (Supplemental Fig. S2).

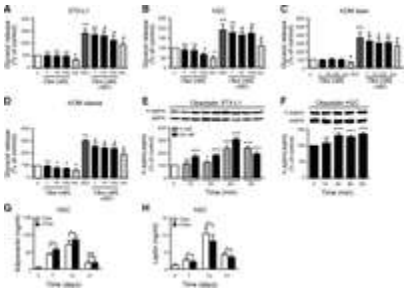

Figure 4.

Obestatin inhibits ISO-induced lipolysis in 3T3-L1 and human adipocytes. A–D) Differentiated 3T3-L1 (A), hSC (B), and hOM adipocytes from lean (C) or obese individuals (D) were incubated for 40 min either with or without obestatin (Obe) at the indicated concentrations or insulin (100 nM). Lipolysis was measured in the absence or presence of 1 μM ISO that was added for a further 80 min. Results are expressed as percentage of glycerol release in basal conditions (control; n=4). *P < 0.05, **P < 0.01 vs. control; #P < 0.05 vs. ISO; ns, not significant. E, F) AMPK phosphorylation, assessed by Western blot in differentiated 3T3-L1 (E) and hSC (F) adipocytes stimulated for the indicated times with obestatin (10 and 100 nM for 3T3-L1 and 10 nM for hSCs) in serum-free medium. Graphs show the densitometric analysis of P-AMPK normalized to AMPK

and reported as percentage of basal. *P < 0.05, ***P < 0.001. G, H) Adiponectin (G) and leptin (H) secretion in hSC adipocytes, assessed at the indicated days of differentiation in either absence or presence of obestatin (10 nM; n=4, triplicate determinations). *P < 0.05.

AMPK has been shown to antagonize ISO-induced lipolysis in both rodent and human adipocytes (29, 30); therefore, we hypothesized that obestatin would activate AMPK. In both 3T3-L1 and hSC adipocytes, obestatin increased AMPK activity, as determined by increased phosphorylation on Thr172. In 3T3-L1, phospho-AMPK was increased by 10 nM and even more by 100 nM obestatin in a time-dependent manner, starting at 15 min (with 100 nM only), peaking at 60 min, and declining thereafter (Fig. 4E); 10 nM, the lowest obestatin concentration showing the best antilipolytic effect, similarly increased phospho-AMPK in hSC adipocytes (from 30 to 90 min; Fig. 4F).

Adiponectin and leptin were shown to exert either antilipolytic or lipolytic actions, respectively (31,–,33). Therefore, we tested obestatin effects on secretion of these adipokines in hSC adipocytes. Figure 4G, H shows that obestatin increased adiponectin secretion at d 7 and 14 of differentiation, whereas it inhibited that of leptin at d 7, 14, and 21.

Obestatin promotes glucose uptake in 3T3-L1 and human adipocytes

To assess obestatin effect on glucose uptake, 3T3-L1 and hSC adipocytes were incubated with obestatin in either absence or presence of insulin. As expected, insulin increased 2-deoxyglucose uptake with respect to control. Obestatin increased insulin-induced glucose uptake at 10 nM and particularly at 100 nM in both 3T3-L1 and hSC cells. Furthermore, 100 nM obestatin stimulated glucose uptake even in the absence of insulin in both cell types, and in hSC cells this effect was equal to that of insulin (Fig. 5A).

Figure 5.

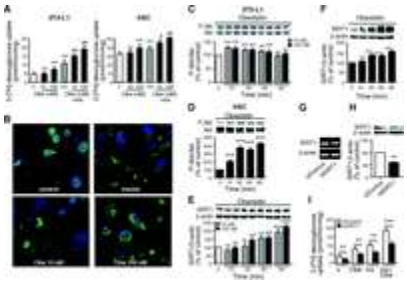

Figure 5.

Obestatin stimulates 2-[3H]-deoxyglucose glucose uptake in 3T3-L1 and hSC adipocytes. A) Differentiated 3T3-L1 and hSC adipocytes incubated in serum-free medium in the absence (control, c) or presence of insulin (ins; 100 nM), either with or without obestatin (Obe) at the indicated concentrations (n=4, duplicate determinations). **P <

0.01 vs. control; ##P < 0.01 vs. ins; ns, not significant. B) Obestatin effects on GLUT-4 accumulation in the plasma membrane. 3T3-L1 preadipocytes were differentiated in chamber slides and then probed for GLUT-4. Insulin was used at 100 nM. Cells were visualized by confocal microscopy (n=3; ×100). C–F) Akt phosphorylation (C, D) and SIRT1 protein expression (E, F) assessed by Western blot in differentiated 3T3-L1 (C, E) and hSC adipocytes (D, F), stimulated for the indicated times with obestatin (10 and 100 nM for 3T3-L1 and 100 nM for hSCs) in serum-free medium. Blots were reprobed with antibody to Akt for P-Akt and to β-actin for SIRT1. Graphs show the densitometric analysis of P-Akt normalized to Akt and SIRT1 to β-actin and reported as percentage of basal (n=3). **P < 0.01, ***P < 0.001 vs. time 0. G) SIRT-1 mRNA assessed by RT-PCR in 3T3-L1 adipocytes after 48 h transfection with either nonsilencing siRNA (siControl) or siRNA to SIRT1 (siSIRT1). As expected, the amplified products corresponded to 369 bp for mouse SIRT1, and 230 bp for β-actin that was used as internal control. H) SIRT1 protein expression assessed by Western blot in 3T3-L1 adipocytes after 48 h transfection with either siControl or siSIRT1. Blots were reprobed with anti-β-actin antibody. Graphs represent the densitometric analysis of SIRT1 normalized to β-actin and reported as percentage of siControl (n=3). **P < 0.01. I) Inhibition of obestatin-induced glucose uptake in 3T3-L1 adipocytes transfected with siSIRT1. 2-[3H]-deoxyglucose glucose uptake was assessed in siControl- or siSIRT1-transfected 3T3-L1 adipocytes incubated in serum-free medium (c) in the absence or presence of insulin (100 nM) and either with or without obestatin (100 nM; n=4). **P < 0.01, ***P < 0.001.

GLUT-4 distribution was examined by confocal microscopy in differentiated 3T3-L1 adipocytes under basal and insulin- and obestatin-stimulated conditions. Compared with untreated cells, which demonstrated diffuse cytoplasmic staining, both insulin and obestatin independently induced GLUT-4 translocation on the cell membrane. Obestatin showed the best effect at 100 nM, where GLUT-4 translocation appeared to be slightly stronger than that induced by insulin at the same concentration, whereas at 10 nM the effect was lower (Fig. 5B). Similar results were obtained in hSC adipocytes (data not shown).

Furthermore, obestatin increased Akt phosphorylation in either differentiated 3T3-L1 or hSC adipocytes. In 3T3-L1 adipocytes, Akt phosphorylation increased at 15 min at both 10 and 100 nM obestatin and declined thereafter, being not significant at 90 min (Fig. 5C). In hSC adipocytes, 100 nM obestatin, the best concentration to promote glucose uptake, increased phospho-Akt from 15 up to 90 min (Fig. 5D).

SIRT1 has been shown to exert anti-inflammatory effects and to increase glucose transport and insulin signaling in adipocytes (34). Therefore, we investigated SIRT1 involvement in obestatin-induced glucose uptake. Obestatin (100 nM) increased SIRT1 protein in 3T3-L1 adipocytes at 30 min; thereafter, both 10 and 100 nM obestatin further up-regulated SIRT1 at 60 and 90 min (Fig. 5E). In hSC adipocytes, SIRT1 similarly increased from 30 to 90 min on obestatin stimulation (100 nM; Fig. 5F). To further assess the role of SIRT1 in obestatin effects on glucose metabolism, we used siRNA targeted to SIRT1 in 3T3-L1 adipocytes. At 48 h after transfection, both SIRT1 mRNA and protein were reduced by siSIRT1 (40% for SIRT1 protein) compared with scrambled siRNA-transfected cells (control; Fig. 5G, H). SIRT1 knockdown decreased glucose

transport in insulin-stimulated cells, and a similar effect was observed in the absence of insulin (control cells), whereas glucose uptake was lower. Obestatin-induced glucose uptake was reduced in siSIRT1 cells as compared with control siRNA both in the absence and, particularly, in the presence of insulin (Fig. 5I).

Obestatin reduces insulin resistance in HFD-fed mice

We next determined whether obestatin would improve the impaired insulin sensitivity induced by short-term treatment with HFD. To this end, 8-wk-old mice were either untreated or intraperitoneally injected with obestatin and fed for 8 wk with HFD or LFD. Body weight was unchanged during HFD as compared with LFD feeding (Fig. 6A), likely because of the short duration of treatment, which mostly causes insulin resistance instead of obesity. Obestatin treatment did not influence body weight at the end of both diets. However, it reduced body weight to a limited extent in both LFD (wk 2 and 5 to 7) and HFD feeding (wk 1 and 2; Fig. 6A). HFD feeding increased organ weight, particularly that of epididymal and SC adipose tissues, with respect to LFD. Obestatin did not influence tissue weight under either diet condition (Supplemental Fig. S2A). As previously shown (24), HFD-fed mice consumed more calories than LFD-fed mice; however, energy intake did not significantly differ between obestatin-treated and untreated mice across diets (Fig. 6B).

Figure 6.

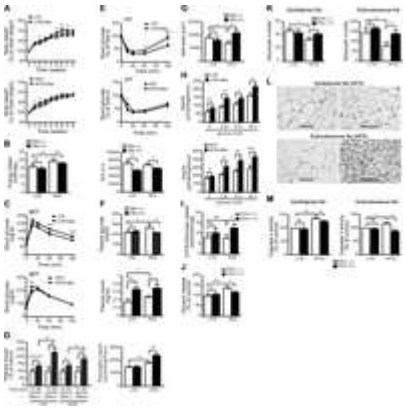

Figure 6.

Obestatin improves the metabolic profile of HFD-fed mice. Mice (8 wk old) were untreated or treated with obestatin (Obe) and fed with either LFD or HFD for 8 wk. A) Body weight measured at the indicated time points in mice fed an LFD (top panel) or an HFD (bottom panel) (n=14 mice/group). B) Energy intake. C) GTT in LFD (top panel) and HFD (bottom panels) control and obestatin-treated mice. D) Insulin levels under nonfeeding conditions, measured from tail vein blood samples collected at 0 and 30 min in GTT. E) Global area AUC for ITT based on absolute glucose levels (mg/dl; n=10 mice/group). F) Plasma glucose, plasma insulin, and pancreatic insulin levels (n=6 mice/group). G) Mean pancreatic islet area evaluated by morphometric analysis in ≥10 islets/condition (n=6 mice/group). H) Glucose-induced insulin secretion during a 60-min incubation in pancreatic islets from LFD-fed mice (top panel) and HFD-fed mice (bottom panel) (n=6 mice/group). I) 2-[3H]-deoxyglucose uptake in epididymal fat explants (n=4

mice/group). J) Lipolysis in epididymal fat explants assessed as glycerol release and expressed as percentage of control (LFD; n=4 mice/group). K) Mean number of adipocytes in epididymal (left panel) and SC (right panel) WAT (n=4 mice/group; ×400). L) Hematoxylin and eosin staining of epididymal or SC fat in mice fed an HFD, either untreated (vehicle) or treated with obestatin (n=4 mice/group). M) Caspase-3 activation, expressed as percentage of control (LFD) assessed in epididymal (left panel) and SC (right panel) fat (n=4). *P < 0.05, **P < 0.01, ***P < 0.001; ns, not significant.

To investigate the consequences of obestatin treatment on glucose homeostasis, GTTs and ITTs were performed in LFD- and HFD-fed control and obestatin-treated mice (Fig. 6C, E). Obestatin-treated mice displayed an improvement in the response to glucose and insulin, as glucose levels remained lower in obestatin-treated mice as compared with their control littermates at both 60 and 120 min postinjection in the LFD group and at 15 min in the HFD group. Area under the curve (AUC) values for ITT revealed better preservation of glucose tolerance of obestatin-treated mice in both LFD and HFD groups compared with controls (Fig. 6E), suggesting that obestatin improves insulin sensitivity (AUC for GTT, based on absolute glucose levels: for LFD-fed control vs. obestatin-treated mice, 20,010±1132 vs. 16,326±737 mg/dl, P<0.05; for HFD-fed control vs. obestatin-treated mice, 19,129±669 vs. 18,193±648 mg/dl). Measurement of insulin levels from tail-vein blood samples collected at 0 and 30 min after glucose injection in GTTs revealed that both LFD- and HFD-fed obestatin-treated mice secreted more insulin than control mice (Fig. 6D).

Obestatin also prevented the negative effect of HFD on glucose homeostasis by reducing plasma glucose to levels comparable to those of LFD (Fig. 6F). Moreover, in HFD-fed mice, obestatin further enhanced plasma and pancreatic insulin, which were both increased in HFD-fed as compared with LFD-fed untreated mice. Obestatin even increased plasma but not pancreatic insulin in LFD-fed mice as compared with untreated mice (Fig. 6F). These results suggested direct insulinotropic effects of obestatin. Indeed, treatment with obestatin, besides counteracting HFD-induced reduction of islet area (Fig. 6G), strongly stimulated glucose-induced insulin secretion in islets explanted from LFD- and, in particular, from HFD-fed mice, at all the glucose concentrations tested. Notably, in untreated mice, either basal or glucose-induced insulin secretion from islets was increased under HFD with respect to LFD feeding (Fig. 6H).

These results, together with those obtained in 3T3-L1 and human adipocytes, prompted us to investigate the obestatin effect on glucose uptake and lipolysis in WAT from LFD- and HFD-fed mice. Figure 6I shows increased 2-deoxyglucose uptake in epididymal fat from obestatin-treated mice fed an HFD with respect to untreated animals, whereas no significant effect was observed in LFD-fed mice. Under insulin-stimulated conditions, glucose uptake increased in explants from both LFD- and HFD-fed mice. Moreover, in fat from obestatin-treated HFD-fed mice, glucose uptake was similar to that of untreated mice stimulated with insulin (Supplemental Fig. S2B). Treatment with obestatin also counteracted HFD-induced lipolysis, as assessed by reduced glycerol release from epididymal fat explants (Fig. 6J).

To further assess the role of obestatin role on adipogenesis and inhibition of apoptosis, we determined adipocyte numbers and morphology, as well as apoptosis, in WAT explants from both LFD- and HFD-fed

mice. HFD-fed mice displayed reduced adipocyte numbers in both epididymal and SC fat explants, as compared with LFD-fed mice (Fig. 6K). Obestatin treatment counteracted the effect of HFD by increasing adipocyte number but had no effect in LFD-fed mice. Accordingly, histological analysis indicated that epididymal and SC fat from HFD-fed mice displayed the expected enlarged, lipid-engorged adipocytes. In contrast, on obestatin treatment, HFD-fed mice showed increased adipocyte numbers with much smaller average cell sizes in both epididymal and, particularly, SC fat (Fig. 6L).

In untreated mice, apoptosis increased in both epididymal and SC fat from HFD-fed mice, as assessed by increased caspase-3 activity. Obestatin counteracted HFD-induced apoptosis in both fat explants, particularly in SC fat (Fig. 6M).

Obestatin levels in plasma from HFD- and LFD-fed mice were similar in both obestatin-treated and untreated animals, as assessed by ELISA (data not shown). Obestatin protein expression was also analyzed in tissues of mice fed a standard diet, being high in the stomach and low in epididymal and perirenal fat. Moreover, preproghrelin mRNA was highly expressed in the stomach of HFD-fed as compared with LFD-fed mice, whereas very low expression was found in adipose tissues under both diet conditions (Supplemental Fig. S3C, D).

Obestatin reduces inflammation in HFD-fed mice

Obestatin counteracted the inhibitory effect of HFD on adiponectin secretion by increasing adiponectin levels in both epididymal and SC adipose tissue (Fig. 7A, B). Moreover, obestatin increased adiponectin levels in SC fat from LFD-fed mice (Fig. 7B). The effects of obestatin on inflammatory cytokine production in adipose tissue, liver, and skeletal muscle of HFD-fed mice were also investigated. Figure 7A, B shows that obestatin reduced TNF-α and IL-1β levels in both epididymal and SC adipose tissue in HFD-fed mice, but not in LFD-fed mice. Similarly, obestatin reduced TNF-α in liver and muscle of HFD-fed mice and blocked IL-1β increase in the liver (Fig. 7C, D). Muscle IL-1β levels were unchanged in mice fed an HFD, and obestatin had no effect on IL-1β secretion in muscle (data not shown).

Figure 7.

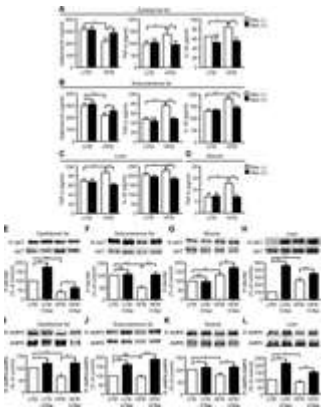

Figure 7.

Obestatin reduces inflammatory cytokine secretion and promotes Akt and AMPK phosphorylation in peripheral tissues of mice fed an HFD. Mice (8 wk old) were untreated or treated with obestatin (Obe) and fed with either LFD or HFD for 8 wk. A, B) Adiponectin, TNF-α, and IL-1β secretion from epididymal fat (A) and SC fat (B). C, D) TNF-α and IL-1β secretion from the liver (C) and TNF-α release from soleus muscle (D); n = 6 mice/group. E–L) Akt (E–H) and AMPK (I–L) phosphorylation (top panels) assessed by Western blot in epididymal fat (E, I), SC fat (F, J), soleus muscle (G, K), and liver (H, L). Blots were reprobed with antibodies to total proteins. Graphs represent the densitometric analysis of phosphorylated proteins normalized to total proteins and reported as percentage of LFD (n=3). *P < 0.05, **P < 0.01, ***P < 0.001; ns, not significant.

Obestatin increases Akt and AMPK phosphorylation in metabolic tissues of HFD-fed mice

Obestatin effects were next determined on Akt and AMPK activation in peripheral tissues. Akt phosphorylation on serine 473 was decreased in epididymal and SC fat of HFD-fed mice, with respect to LFD-fed mice (Fig. 7E, F). Conversely, phospho-Akt increased in muscle and liver of HFD-fed as compared with LFD-fed mice (Fig. 7G, H). Obestatin increased phospho-Akt in fat, muscle, and liver of HFD-fed mice (Fig. 7E–H) and in epididymal fat and liver of LFD-fed mice (Fig. 7E, H). Similarly, in fat, muscle, and liver, obestatin counteracted HFD-induced reduction of phopsho-AMPK and even increased phopsho-AMPK in LFD-fed mice (Fig. 7I–L).

DISCUSSION

This study shows that obestatin regulates adipocyte function and glucose metabolism. Obestatin, which is released by and binds to mouse and human adipocytes, inhibits preadipocyte apoptosis, counteracts ISO-induced lipolysis, promotes glucose uptake and GLUT4 translocation, stimulates adiponectin, and inhibits leptin secretion. In HFD-fed mice, obestatin reduces insulin resistance and inflammation and activates key metabolic signaling pathways in WAT, liver, and muscle.

WAT has a multifarious composition, comprising preadipocytes, adipocytes, macrophages, endothelial cells, fibroblasts, and leukocytes, which render this tissue an important mediator of metabolism and inflammation. Since the discovery of leptin, WAT has been recognized as an endocrine organ, secreting multiple adipokines, including hormone-like proteins and inflammatory cytokines (1,–,3). Many of these adipokines were originally described as being produced by tissues other than WAT. This is also the case of obestatin, which is mainly produced by the stomach but also the pancreas and other peripheral tissues (13, 14). Here, we first show obestatin secretion from mouse 3T3-L1 and human SC and OM adipocytes in both undifferentiated and differentiated cells. This finding suggests that obestatin may be a novel adipokine, exerting either local autocrine/paracrine or distant endocrine effects. Adipokines, besides having broad actions in the body, regulate pancreatic β-cell function, including insulin secretion, gene expression, and apoptosis (35). Therefore, based on our present and previous findings in the endocrine pancreas (11, 16), it cannot be excluded that adipose tissue-derived obestatin may also influence pancreatic function. That adipocyte-derived obestatin may display autocrine/paracrine functions is also supported by previous

studies showing that both inhibition of preproghrelin expression and neutralization of preproghrelin-derived peptides, including obestatin, reduce adipocyte differentiation (20, 36). Here, the obestatin effect on adipocyte differentiation was less relevant, as compared with other functions, such as inhibition of lipolysis, induction of glucose uptake, regulation of β-cell function, or inhibition of inflammation. Therefore, the autocrine/paracrine functions of obestatin may be related to these aspects. Interestingly, obestatin protein and preproghrelin mRNA were found here to be expressed in mouse epididymal and subcutaneous adipose tissues, although their levels in fat were much lower than those in the stomach. Furthermore, preproghrelin mRNA expression in the stomach of HFD-fed mice was much higher than that of LFD-fed mice, consistent with previous studies (37, 38).

That GPR39 is the obestatin receptor is still strongly debated (4, 7), and GPR39 expression in both mouse and human adipocytes has already been demonstrated (17, 20, 36). However, we previously suggested that obestatin at least partly interacts with GLP-1R in pancreatic β cells, which would explain to some extent its insulinotropic and survival effects (11). Here, obestatin binding to 3T3-L1 and human adipocytes was found displaced by the GLP-1R agonist Ex-4 and antagonist Ex-9; moreover, reducing the expression of GLP-1R in 3T3-L1 preadipocytes and adipocytes by siGLP-1R prevented obestatin binding to these cells. Therefore, as for β cells, obestatin may trigger survival and metabolic signaling pathways through interaction with GLP-1R. Consistently, recent findings have highlighted the role of GLP-1R in adipogenesis, adipocyte proliferation, and apoptosis (39), and GLP-1R mRNA expression was found here to increase during adipocyte differentiation. Conversely, obestatin showed no effect on GLP-1R expression.

Obestatin binding in preadipocytes suggested effects in undifferentiated cells. Indeed, we first showed that obestatin prevents apoptosis and increases survival of 3T3-L1 preadipocytes. As for other cell types (10, 11), obestatin antiapoptotic effects in preadipocytes involved activation of ERK1/2 and PI3K/Akt, which play a key role in adipocyte proliferation and survival (40,–,42). Adipocyte cell death is an event that may be enhanced by obesity or secondary to inflammation and macrophage infiltration (2, 3). Here, obestatin treatment in HFD-fed mice reduced WAT apoptosis, besides decreasing systemic inflammation.

Adipose tissue remodeling is an ongoing physiological process involving both adipose cell apoptosis and adipogenesis. The latter implies the sequential induction of multiple transcription factors, acquisition of specific metabolic competences, and ability to produce and secrete fat-specific proteins. Deregulation of adipogenesis can contribute to obesity or lipodystrophy. However, adipocytes represent a safe place to store lipids, and enhanced adipogenesis, rather than being a cause of obesity, is the result of imbalance between energy intake and energy output (43). In the present study, obestatin enhanced TG content in differentiating 3T3-L1 and hSC adipocytes and increased adipogenesis in hOM adipocytes obtained from obese but not from lean individuals. OM fat, which mostly contributes to the pathogenesis of insulin resistance and T2D (44), is morphologically and functionally different from SC fat. Indeed, fat cells from different depots vary in size and responses to insulin and lipolytic agents, lipoprotein binding, fatty acid transfer, and production of secreted proteins (45). Such differences could contribute to the distinct effects of hormones on SC compared with OM fat. Here, adipogenesis was found to be greater in hSC than in hOM adipocytes, consistent with previous findings (46); similarly, the obestatin adipogenic effect was stronger in hSC than in hOM fat cells. Interestingly, AG and UAG were previously found to increase differentiation in

3T3-L1 cells and cultured human adipocytes (41, 47), and obestatin showed similar effects in 3T3-L1 cells (19, 20), indicating adipogenic actions of all the ghrelin gene-derived peptides.

Catecholamines are the most potent regulators of lipolysis in human adipocytes, and OM fat cells, particularly in obese individuals, have higher lipolytic activity than SC adipocytes, contributing to the increased free fatty acid levels in the systemic circulation (45). This is consistent with our present findings showing lower ISO-induced lipolysis in SC than in OM adipocytes; moreover, OM adipocyte lipolysis was reduced in obese with respect to lean individuals. Lipolysis is inhibited by insulin, which has a stronger effect in hSC than in hOM adipocytes (48). Obestatin was found here to inhibit ISO-induced lipolysis in both 3T3-L1 and human adipocytes. Interestingly, like insulin, obestatin inhibited lipolysis even in the absence of ISO in both SC and OM adipocytes of obese individuals. Conversely, the other ghrelin gene-derived peptides ghrelin and UAG showed no effect on obestatin antilipolytic action, as indicated by coincubation experiments in 3T3-L1 adipocytes. In support of its antilipolytic role, obestatin also increased the phosphorylation of AMPK. This is an energy sensor that controls whole-body glucose homeostasis by regulating metabolism in peripheral tissues, and its activity has been shown to counteract ISO-induced lipolysis in both rodent and human adipocytes (29, 30). AMPK activation also increases glucose uptake and metabolism, fatty acid oxidation, and inhibition of hepatic lipogenesis and glucose production (49). Therefore, the finding that obestatin activates AMPK further substantiates its positive metabolic role.

Obestatin increased adiponectin and reduced leptin secretion from hSC adipocytes. Notably, besides its insulin-sensitizing effects, adiponectin activates AMPK in metabolic tissues and inhibits adipocyte lipolysis (31). Conversely, leptin impairs insulin metabolic actions in adipocytes, i.e., stimulation of glucose transport, lipogenesis, and inhibition of ISO-induced lipolysis (32, 33). Overall, these results indicate that besides increasing adipogenesis, obestatin prevents lipolysis and acts similarly to insulin, although less potently; moreover, its actions in adipocytes at least partly resemble those of AG and UAG, which were found to increase adipogenesis in vivo and to inhibit ISO-induced lipolysis in vitro (50,–,52).

With regard to glucose metabolism, we found that obestatin stimulated glucose uptake per se and enhanced the effect of insulin in both 3T3-L1 and hSC adipocytes. Interestingly, the obestatin effect was comparable to that of insulin when the peptides were used at equal concentrations in hSC adipocytes. In these experiments, only hSC cells were used, mainly because of the elevated number of cells required, which could not be obtained from small visceral biopsies.

GLUT4 is the major insulin-responsive GLUT for insulin-dependent glucose disposal. Transgenic mice overexpressing GLUT4 in adipose tissue or skeletal muscle are highly insulin sensitive and glucose tolerant, whereas heterozygous GLUT4-knockout mice in muscle and adipose tissue show insulin resistance and diabetes (53). GLUT4 has an intracellular disposition in the unstimulated state and is redistributed to the plasma membrane in response to insulin and other stimuli (54). Here, obestatin promoted GLUT4 translocation to the plasma membrane in 3T3-L1 adipocytes. This effect was at least as strong as that of insulin, suggesting that obestatin may influence GLUT4 translocation and glucose uptake independently of insulin.

We have recently demonstrated that obestatin induces Akt phosphorylation in pancreatic β cells and activates downstream targets of insulin (11). In adipocytes, PI3K/Akt activity is essential for insulin-stimulated glucose transport and GLUT4 translocation to the cell membrane (42, 54). In the present study, obestatin per se stimulated Akt phosphorylation in mice and hSC adipocytes, further suggesting insulin-like effects.

Activation of the NAD-dependent histone deacetylase SIRT1 in adipocytes increases glucose uptake and insulin signaling, reduces expression of inflammatory genes, and protects against HFD-induced metabolic damage (34, 55). Obestatin increased SIRT1 protein in both 3T3-L1 and hSC adipocytes, possibly acting as a SIRT1 activator. Moreover, SIRT1 knockdown in 3T3-L1 adipocytes strongly inhibited obestatin-induced glucose uptake, in either absence or presence of insulin, suggesting that SIRT1 is involved in obestatin-induced glucose uptake. However, obestatin does not parallel all SIRT1 actions. Indeed, at variance with the obestatin adipogenic and antilipolytic effects, SIRT1 has been previously shown to repress differentiation and to stimulate lipolysis (56). Likely, in adipocytes obestatin activates additional signaling pathways or second-messenger cross-talk, similar to those observed in β cells (11). Moreover, obestatin and SIRT1 may influence the secretion of different adipokines, adding further complexity to the system. For instance, SIRT1 stimulates adiponectin release, which in turn increases insulin sensitivity (56).

Based on the observed insulin-like and insulin-sensitizing effects in adipocytes, we hypothesized that obestatin would exert protective effects against insulin resistance and inflammation in HFD-fed mice. Mice were fed an LFD or an HFD for 8 wk, which is sufficient for inducing insulin resistance, glucose intolerance, and inflammation (57, 58). Obestatin was claimed to exert anorectic effects, opposing the AG orexigenic actions (4); however, obestatin-induced inhibition of food intake has not been confirmed, and its role in feeding and body weight is still unclear (12). Here, treatment with obestatin slightly but not significantly reduced energy intake in both LFD and HFD feeding. Moreover, although obestatin decreased body weight to some extent in both diet groups, no difference was found between treated and untreated groups at wk 8. These findings are consistent with recent studies showing no weight variation in HFD-fed rats treated with obestatin (59).

In HFD-fed mice, obestatin treatment improved insulin sensitivity and reduced glucose intolerance, as suggested by the GTT and ITT results and by reduced plasma glucose levels. Interestingly, plasma insulin levels 30 min after a glucose bolus were significantly higher in obestatin-treated than in control mice, suggesting that β cells from obestatin-treated mice are more sensitive than those from control mice in response to a GTT. Moreover, the fact that the responses to ITT of both LFD and HFD obestatin-treated mice are significantly improved as compared with control mice (and as is clearly indicated by the AUC) suggests that obestatin improves insulin sensitivity. Furthermore, insulin levels after a glucose bolus at 30 min were higher in mice treated with obestatin with respect to untreated mice in both diet conditions, likely explaining why obestatin-treated mice clear circulating glucose faster than controls in response to a GTT.

These results, and the finding that obestatin further increased plasma and pancreatic insulin in HFD and even increased plasma insulin in LFD-fed mice, suggested insulinotropic effects of the hormone. Indeed, obestatin-treated mice showed increased insulin secretion in glucose-stimulated explanted islets from both diet conditions, particularly in HFD, where insulin secretion was increased, consistent with previous studies (57). In addition, obestatin increased islet area in HFD-fed mice, which was reduced as compared with LFD-fed mice. Thus, together with our previous findings in β cells, human pancreatic islets, and animal models of type 1 diabetes (11, 16), these results further support the insulinotropic role of obestatin.

The positive role of obestatin on glucose homeostasis is further sustained by the results obtained in adipose tissue explants from HFD-fed mice, where obestatin treatment increased glucose uptake and reduced lipolysis. In addition, obestatin increased the number of small, likely insulin-sensitive, adipocytes in epididymal and particularly in SC fat of HFD mice. Interestingly, recent studies have shown that increased adipocyte cell numbers and overall expansion of SC adipose tissue mass protect against diet-induced insulin resistance (60).

Adiponectin is known to improve insulin sensitivity by increasing energy expenditure and fatty acid oxidation. Individuals with T2D often exhibit decreased adiponectin levels, and insulin sensitivity is improved by adiponectin therapy (31). In HFD-fed mice, obestatin counteracted adiponectin decrease in WAT and even increased adiponectin in SC fat from LFD-fed mice, further supporting the positive role of obestatin on insulin sensitivity.

Obesity, insulin resistance, and T2D are associated with chronic inflammation and abnormal cytokine production, which seems to be triggered by and reside predominantly in adipose tissue. Among proinflammatory cytokines that are detrimental to insulin effects are TNF-α and IL-1β, which act in an autocrine or paracrine manner to interfere with insulin signaling in peripheral tissues and macrophages (2, 3). Here, obestatin completely blocked HFD-induced TNF-α increase in WAT, liver, and muscle and similarly reduced IL-1β in WAT and liver. Therefore, the alleviated insulin resistance observed in obestatin-treated mice fed an HFD may also result from reduced inflammation in peripheral tissues.

Finally, obestatin increased Akt and AMPK phosphorylation in WAT, muscle and liver of HFD-fed mice and even increased AMPK activity in LFD-fed mice. Interestingly, in untreated HFD-fed mice, phospho-Akt was reduced in epididymal and SC fat, being enhanced in muscle and liver, possibly because of compensatory mechanisms or increased insulin levels that stimulated PI3K/Akt signaling. Akt and AMPK play a key role in peripheral insulin sensitivity, and their activity is reduced in humans and in animal models of insulin resistance (42, 49). Consistent with our findings, decreased AMPK activity has been observed in adipose tissue and isolated adipocytes of mice fed an HFD (61), and AMPK activation in mice increases systemic insulin sensitivity and protects from HFD-induced obesity and inflammation (49).

Previous results from a single study (20) have reported obestatin effects on adipocytes, which were found to be similar to our findings. However, at variance with that study, which only examined mouse and rat adipocytes, this study describes obestatin effects in human primary OM and SC adipocytes. Moreover, we provide additional evidence of signaling mechanisms triggered by and involved in obestatin metabolic effects, such as GLP-1R, which is likely bound by the peptide AMPK, which was previously found not to be activated by obestatin (20), and SIRT-1, which is shown here to be involved in obestatin-induced glucose uptake. We also first report obestatin effects on adiponectin and leptin secretion in vitro and on inhibition of inflammation in vivo. Furthermore, we tested the effects of obestatin in a mouse model of diet-induced insulin resistance, providing strong and novel evidence of the positive metabolic role of this peptide. Conversely, in the previous studies these aspects were not considered, and, to our knowledge, there is no evidence of other studies showing such effects. Therefore, the present study, when compared with others, investigates the effects of obestatin in much more in detail not only in vitro; most notably, this is the first report showing the effect of obestatin in vivo, using an animal model of insulin resistance.

Overall, our findings suggest a novel role of obestatin in adipocyte function and glucose metabolism. Obestatin is produced in mouse and human adipocytes and promotes preadipocyte cell survival and influences lipolysis and glucose uptake in vitro. In vivo, obestatin reduces insulin resistance and systemic inflammation in HFD-fed mice. Together with our previous findings in the endocrine pancreas, these results further indicate the relevant metabolic role of obestatin and suggest potential therapeutic perspectives in insulin resistance and metabolic dysfunctions.

Acknowledgments

The authors thank Amalia Bosia, Stefano Bruschi, Francesco Ferrini, Rhonda Kineman, Roberto Gambino, Fabio Malavasi, Adalberto Merighi, Susanna Romboli, Ana I. Pozo-Salas, Roy G. Smith, Marina Taliano, Letizia Trovato, and Alicia Villa-Osaba for contributing to the study.

This work was supported by the following grants: Regione Piemonte 2008, Brain Drain University of Turin 2008, and Ministro dell'Istruzione, dell'Università e della Ricerca 2009 (to R.G.); Compagnia di San Paolo 2008 (to E.G.); Ministerio de Ciencia e Innovación/Fonds Européen de Développement Régional RYC-2007-00186, BFU2008-01136/BFI (to R.M.L.); Instituto de Salud Carlos III FI06/00804 (to J.C.C.); and BFU2010-19300 and CTS-5051 (to J.P.C.); and by the Studio delle Malattie Endocrino Metaboliche Foundation (Turin, Italy). Centro de Investigación Biomédica en Red de Fisiopatología de la Obesidad y Nutrición is an initiative of Instituto de Salud Carlos III.

This article includes supplemental data. Please visit http://www.fasebj.org to obtain this information.

Abbreviations:

AG

acylated ghrelin

AMPK

AMP-activated protein kinase

AUC

area under the curve

DM

differentiation medium

EIA

enzyme immunoassay

ERK1/2

extracellular signal-regulated kinase

Ex-4

exendin-4

Ex-9

exendin-9

GLP-1R

glucagon-like peptide 1 receptor

GLUT4

glucose transporter type 4

GPR39

G-protein-coupled receptor 39

GTT

glucose tolerance test

HFD

high-fat diet

hOM

human omental

hSC

human subcutaneous

IBMX

3-isobutyl-1-methylxanthine

IGF-I

insulin-like growth factor I

IL-1β

interleukin-1β

ISO

isoproterenol

ITT

insulin tolerance test

LFD

low fat diet

OM

omental

PI3K

phosphoinositide 3-kinase

RIA

radioimmunoassay

SC

subcutaneous

siRNA

small interfering RNA

SIRT1

sirtuin 1

T2D

type 2 diabetes

TG

triglyceride

TNF-α

tumor necrosis factor α

UAG

unacylated ghrelin

WAT

white adipose tissue

References

1.↵ Ahima R. S., Flier J. S. (2000) Adipose tissue as an endocrine organ. Trends Endocrinol. Metab. 11, 327–332 CrossRefMedline

2.↵ Hotamisligil G. S. (2006) Inflammation and metabolic disorders. Nature 444, 860–867 CrossRefMedline

3.↵ Schenk S., Saberi M., Olefsky J. M. (2008) Insulin sensitivity: modulation by nutrients and inflammation. J. Clin. Invest. 118, 2992–3002 CrossRefMedline

4.↵ Zhang J. V., Ren P. G., Avsian-Kretchmer O., Luo C. W., Rauch R., Klein C., Hsueh A. J. (2005) Obestatin, a peptide encoded by the ghrelin gene, opposes ghrelin's effects on food intake. Science 310, 996–999

5.↵ Ataka K., Inui A., Asakawa A., Kato I., Fujimiya M. (2008) Obestatin inhibits motor activity in the antrum and duodenum in the fed state of conscious rats. Am. J. Physiol. Gastrointest. Liver Physiol. 294, G1210–G1218

6.↵ Zhang J. V., Jahr H., Luo C. W., Klein C., Van Kolen K., Ver Donck L., De A., Baart E., Li J., Moechars D., Hsueh A. J. (2008) Obestatin induction of early-response gene expression in gastrointestinal and adipose tissues and the mediatory role of G protein-coupled receptor, GPR39. Mol. Endocrinol. 22, 1464–1475

7.↵ Chartrel N., Alvear-Perez R., Leprince J., Iturrioz X., Reaux-Le Goazigo A., Audinot V., Chomarat P., Coge F., Nosjean O., Rodriguez M., Galizzi J. P., Boutin J. A., Vaudry H., Llorens-Cortes C. (2007) Comment on “Obestatin, a peptide encoded by the ghrelin gene, opposes ghrelin's effects on food intake.” Science 315, 766; author reply 766

8.↵ Holst B., Egerod K. L., Schild E., Vickers S. P., Cheetham S., Gerlach L. O., Storjohann L., Stidsen C. E., Jones R., Beck-Sickinger A. G., Schwartz T. W. (2007) GPR39 signaling is stimulated by zinc ions but not by obestatin. Endocrinology 148, 13–20

9.↵ Tremblay F., Perreault M., Klaman L. D., Tobin J. F., Smith E., Gimeno R. E. (2007) Normal food intake and body weight in mice lacking the G protein-coupled receptor GPR39. Endocrinology 148, 501–506

10.↲ Alloatti G., Arnoletti E., Bassino E., Penna C., Perrelli M. G., Ghe C., Muccioli G. (2010) Obestatin affords cardioprotection to the ischemic-reperfused isolated rat heart and inhibits apoptosis in cultures of similarly stressed cardiomyocytes. Am. J. Physiol. Heart Circ. Physiol. 299, H470–H481

11.↲ Granata R., Settanni F., Gallo D., Trovato L., Biancone L., Cantaluppi V., Nano R., Annunziata M., Campiglia P., Arnoletti E., Ghe C., Volante M., Papotti M., Muccioli G., Ghigo E. (2008) Obestatin promotes survival of pancreatic beta-cells and human islets and induces expression of genes involved in the regulation of beta-cell mass and function. Diabetes 57, 967–979

12.↲ Seim I., Walpole C., Amorim L., Josh P., Herington A., Chopin L. (2012) The expanding roles of the ghrelin-gene derived peptide obestatin in health and disease. Mol. Cell. Endocrinol. 340, 111

13.↲ Granata R., Baragli A., Settanni F., Scarlatti F., Ghigo E. (2010) Unraveling the role of the ghrelin gene peptides in the endocrine pancreas. J. Mol. Endocrinol. 45, 107–118

14.↲ Gronberg M., Tsolakis A. V., Magnusson L., Janson E. T., Saras J. (2008) Distribution of obestatin and ghrelin in human tissues: immunoreactive cells in the gastrointestinal tract, pancreas, and mammary glands. J. Histochem. Cytochem. 56, 793–801

15.↲ Volante M., Rosas R., Ceppi P., Rapa I., Cassoni P., Wiedenmann B., Settanni F., Granata R., Papotti M. (2009) Obestatin in human neuroendocrine tissues and tumours: expression and effect on tumour growth. J. Pathol. 218, 458–466

16.↲ Granata R., Volante M., Settanni F., Gauna C., Ghe C., Annunziata M., Deidda B., Gesmundo I., Abribat T., van der Lely A. J., Muccioli G., Ghigo E., Papotti M. (2010) Unacylated ghrelin and obestatin increase islet cell mass and prevent diabetes in streptozotocin-treated newborn rats. J. Mol. Endocrinol. 45, 9–17

17.↲ Catalan V., Gomez-Ambrosi J., Rotellar F., Silva C., Gil M. J., Rodriguez A., Cienfuegos J. A., Salvador J., Fruhbeck G. (2007) The obestatin receptor (GPR39) is expressed in human adipose tissue and is down-regulated in obesity-associated type 2 diabetes mellitus. Clin. Endocrinol. (Oxf.) 66, 598–601

18.↲ Egerod K. L., Holst B., Petersen P. S., Hansen J. B., Mulder J., Hokfelt T., Schwartz T. W. (2007) GPR39 splice variants versus antisense gene LYPD1: expression and regulation in gastrointestinal tract, endocrine pancreas, liver, and white adipose tissue. Mol. Endocrinol. 21, 1685–1698

19.↲ Miegueu P., St Pierre D., Broglio F., Cianflone K. (2011) Effect of desacyl ghrelin, obestatin and related peptides on triglyceride storage, metabolism and GHSR signaling in 3T3-L1 adipocytes. J. Cell. Biochem. 112, 704–714

20.↲ Gurriaran-Rodriguez U., Al-Massadi O., Roca-Rivada A., Crujeiras A. B., Gallego R., Pardo M., Seoane L. M., Pazos Y., Casanueva F. F., Camina J. P. (2011) Obestatin as a regulator of adipocyte metabolism and adipogenesis. J. Cell. Mol. Med. 15, 1927–1940

21.↲ Hauner H., Entenmann G., Wabitsch M., Gaillard D., Ailhaud G., Negrel R., Pfeiffer E. F. (1989) Promoting effect of glucocorticoids on the differentiation of human adipocyte precursor cells cultured in a chemically defined medium. J. Clin. Invest. 84, 1663–1670

22.↲ Granata R., Settanni F., Biancone L., Trovato L., Nano R., Bertuzzi F., Destefanis S., Annunziata M., Martinetti M., Catapano F., Ghe C., Isgaard J., Papotti M., Ghigo E., Muccioli G. (2007) Acylated and unacylated ghrelin promote proliferation and inhibit apoptosis of pancreatic beta-cells and human islets: involvement of 3′,5′-cyclic adenosine monophosphate/protein kinase A, extracellular signal-regulated kinase 1/2, and phosphatidyl inositol 3-kinase/Akt signaling. Endocrinology 148, 512–529

23.↲ Mulumba M., Jossart C., Granata R., Gallo D., Escher E., Ghigo E., Servant M. J., Marleau S., Ong H. (2010) GPR103b functions in the peripheral regulation of adipogenesis. Mol. Endocrinol. 24, 1615–1625

24.↲ Luque R. M., Lin Q., Cordoba-Chacon J., Subbaiah P. V., Buch T., Waisman A., Vankelecom H., Kineman R. D. (2011) Metabolic impact of adult-onset, isolated, growth hormone deficiency (AOiGHD) due to destruction of pituitary somatotropes. PLoS ONE 6, e15767

25.↲ Irako T., Akamizu T., Hosoda H., Iwakura H., Ariyasu H., Tojo K., Tajima N., Kangawa K. (2006) Ghrelin prevents development of diabetes at adult age in streptozotocin-treated newborn rats. Diabetologia 49, 1264–1273

26.↲ Adeghate E., Ponery A. S. (2002) Ghrelin stimulates insulin secretion from the pancreas of normal and diabetic rats. J. Neuroendocrinol. 14, 555–560

27.↲ Bonzon-Kulichenko E., Fernandez-Agullo T., Molto E., Serrano R., Fernandez A., Ros M., Carrascosa J. M., Arribas C., Martinez C., Andres A., Gallardo N. (2011) Regulation of insulin-stimulated glucose uptake in rat white adipose tissue upon chronic central leptin infusion: effects on adiposity. Endocrinology 152, 1366–1377

28.↲ Nishiumi S., Bessyo H., Kubo M., Aoki Y., Tanaka A., Yoshida K., Ashida H. (2010) Green and black tea suppress hyperglycemia and insulin resistance by retaining the expression of glucose transporter 4 in muscle of high-fat diet-fed C57BL/6J mice. J. Agric. Food Chem. 58, 12916–12923

29.↲ Bourron O., Daval M., Hainault I., Hajduch E., Servant J. M., Gautier J. F., Ferre P., Foufelle F. (2010) Biguanides and thiazolidinediones inhibit stimulated lipolysis in human adipocytes through activation of AMP-activated protein kinase. Diabetologia 53, 768–778

30.↲ Daval M., Diot-Dupuy F., Bazin R., Hainault I., Viollet B., Vaulont S., Hajduch E., Ferre P., Foufelle F. (2005) Anti-lipolytic action of AMP-activated protein kinase in rodent adipocytes. J. Biol. Chem. 280, 25250–25257

31.↲ Kadowaki T., Yamauchi T., Kubota N., Hara K., Ueki K., Tobe K. (2006) Adiponectin and adiponectin receptors in insulin resistance, diabetes, and the metabolic syndrome. J. Clin. Invest. 116, 1784–1792

32.↲ Muller G., Ertl J., Gerl M., Preibisch G. (1997) Leptin impairs metabolic actions of insulin in isolated rat adipocytes. J. Biol. Chem. 272, 10585–10593

33.↲ Siegrist-Kaiser C. A., Pauli V., Juge-Aubry C. E., Boss O., Pernin A., Chin W. W., Cusin I., Rohner-Jeanrenaud F., Burger A. G., Zapf J., Meier C. A. (1997) Direct effects of leptin on brown and white adipose tissue. J. Clin. Invest. 100, 2858–2864

34.↲ Yoshizaki T., Milne J. C., Imamura T., Schenk S., Sonoda N., Babendure J. L., Lu J. C., Smith J. J., Jirousek M. R., Olefsky J. M. (2009) SIRT1 exerts anti-inflammatory effects and improves insulin sensitivity in adipocytes. Mol. Cell. Biol. 29, 1363–1374

35.↲ Zhao Y. F., Feng D. D., Chen C. (2006) Contribution of adipocyte-derived factors to beta-cell dysfunction in diabetes. Int. J. Biochem. Cell Biol. 38, 804–819

36.↲ Gurriaran-Rodriguez U., Al-Massadi O., Crujeiras A. B., Mosteiro C. S., Amil-Diz M., Beiroa D., Nogueiras R., Seoane L. M., Gallego R., Pazos Y., Casanueva F. F., Camina J. P. (2011) Preproghrelin expression is a key target for insulin action on adipogenesis. J. Endocrinol. 210, R1–7

37.↲ Morash M. G., Gagnon J., Nelson S., Anini Y. (2010) Tissue distribution and effects of fasting and obesity on the ghrelin axis in mice. Regul. Pept. 163, 62–73

38.↲ Wang Z. Q., Zuberi A. R., Zhang X. H., Macgowan J., Qin J., Ye X., Son L., Wu Q., Lian K., Cefalu W. T. (2007) Effects of dietary fibers on weight gain, carbohydrate metabolism, and gastric ghrelin gene expression in mice fed a high-fat diet. Metabolism 56, 1635–1642

39.↲ Challa T. D., Beaton N., Arnold M., Rudofsky G., Langhans W., Wolfrum C. (2012) Regulation of adipocyte formation by GLP-1/GLP-1R signaling. J. Biol. Chem. 287, 6421–6430

40.↲ Boney C. M., Gruppuso P. A., Faris R. A., Frackelton A. R. Jr.. (2000) The critical role of Shc in insulin-like growth factor-I-mediated mitogenesis and differentiation in 3T3-L1 preadipocytes. Mol. Endocrinol. 14, 805–813

41.↲ Kim M. S., Yoon C. Y., Jang P. G., Park Y. J., Shin C. S., Park H. S., Ryu J. W., Pak Y. K., Park J. Y., Lee K. U., Kim S. Y., Lee H. K., Kim Y. B., Park K. S. (2004) The mitogenic and antiapoptotic actions of ghrelin in 3T3-L1 adipocytes. Mol. Endocrinol. 18, 2291–2301

42.↲ Manning B. D., Cantley L. C. (2007) AKT/PKB signaling: navigating downstream. Cell 129, 1261–1274

43.↲ Rosen E. D., MacDougald O. A. (2006) Adipocyte differentiation from the inside out. Nat. Rev. Mol. Cell Biol. 7, 885–896

44.↲ Perrini S., Laviola L., Cignarelli A., Melchiorre M., De Stefano F., Caccioppoli C., Natalicchio A., Orlando M. R., Garruti G., De Fazio M., Catalano G., Memeo V., Giorgino R., Giorgino F. (2008) Fat depot-related differences in gene expression, adiponectin secretion, and insulin action and signalling in human adipocytes differentiated in vitro from precursor stromal cells. Diabetologia 51, 155–164

45.↲ Wajchenberg B. L. (2000) Subcutaneous and visceral adipose tissue: their relation to the metabolic syndrome. Endocr. Rev. 21, 697–738

46.↲ Adams M., Montague C. T., Prins J. B., Holder J. C., Smith S. A., Sanders L., Digby J. E., Sewter C. P., Lazar M. A., Chatterjee V. K., O'Rahilly S. (1997) Activators of peroxisome proliferator-activated receptor gamma have depot-specific effects on human preadipocyte differentiation. J. Clin. Invest. 100, 3149–3153

47.↲ Rodriguez A., Gomez-Ambrosi J., Catalan V., Gil M. J., Becerril S., Sainz N., Silva C., Salvador J., Colina I., Fruhbeck G. (2009) Acylated and desacyl ghrelin stimulate lipid accumulation in human visceral adipocytes. Int. J. Obes. (Lond.) 33, 541–552

48.↲ Giorgino F., Laviola L., Eriksson J. W. (2005) Regional differences of insulin action in adipose tissue: insights from in vivo and in vitro studies. Acta Physiol. Scand. 183, 13–30

49.↲ Fogarty S., Hardie D. G. (2010) Development of protein kinase activators: AMPK as a target in metabolic disorders and cancer. Biochim. Biophys. Acta 1804, 581–591 Medline

50.↲ Muccioli G., Pons N., Ghe C., Catapano F., Granata R., Ghigo E. (2004) Ghrelin and des-acyl ghrelin both inhibit isoproterenol-induced lipolysis in rat adipocytes via a non-type 1a growth hormone secretagogue receptor. Eur. J. Pharmacol. 498, 27–35

51.↲ Thompson N. M., Gill D. A., Davies R., Loveridge N., Houston P. A., Robinson I. C., Wells T. (2004) Ghrelin and des-octanoyl ghrelin promote adipogenesis directly in vivo by a mechanism independent of the type 1a growth hormone secretagogue receptor. Endocrinology 145, 234–242

52.↲ Baragli A., Ghe C., Arnoletti E., Granata R., Ghigo E., Muccioli G. (2011) Acylated and unacylated ghrelin attenuate isoproterenol-induced lipolysis in isolated rat visceral adipocytes through activation of phosphoinositide 3-kinase gamma and phosphodiesterase 3B. Biochim. Biophys. Acta 1811, 386–396

53.↲ Minokoshi Y., Kahn C. R., Kahn B. B. (2003) Tissue-specific ablation of the GLUT4 glucose transporter or the insulin receptor challenges assumptions about insulin action and glucose homeostasis. J. Biol. Chem. 278, 33609–33612

54.↲ Huang S., Czech M. P. (2007) The GLUT4 glucose transporter. Cell Metab. 5, 237–252 CrossRefMedline 55.↲ Pfluger P. T., Herranz D., Velasco-Miguel S., Serrano M., Tschop M. H. (2008) Sirt1 protects against high-fat diet-induced metabolic damage. Proc. Natl. Acad. Sci. U. S. A. 105, 9793–9798

56.↲ Liang F., Kume S., Koya D. (2009) SIRT1 and insulin resistance. Nat. Rev. Endocrinol. 5, 367–373

57.↲ Reimer M. K., Ahren B. (2002) Altered beta-cell distribution of pdx-1 and GLUT-2 after a short-term challenge with a high-fat diet in C57BL/6J mice. Diabetes 51(Suppl. 1), S138–143

58.↲ Wueest S., Rapold R. A., Schumann D. M., Rytka J. M., Schildknecht A., Nov O., Chervonsky A. V., Rudich A., Schoenle E. J., Donath M. Y., Konrad D. (2010) Deletion of Fas in adipocytes relieves adipose tissue inflammation and hepatic manifestations of obesity in mice. J. Clin. Invest. 120, 191–202

59.↲ Brunetti L., Leone S., Orlando G., Recinella L., Ferrante C., Chiavaroli A., Di Nisio C., Di Michele P., Vacca M. (2009) Effects of obestatin on feeding and body weight after standard or cafeteria diet in the rat. Peptides 30, 1323–1327

60.↲ Kim J. Y., van de Wall E., Laplante M., Azzara A., Trujillo M. E., Hofmann S. M., Schraw T., Durand J. L., Li H., Li G., Jelicks L. A., Mehler M. F., Hui D. Y., Deshaies Y., Shulman G. I., Schwartz G. J., Scherer P. E. (2007) Obesity-associated improvements in metabolic profile through expansion of adipose tissue. J. Clin. Invest. 117, 2621–2637

61.↵ Gaidhu M. P., Anthony N. M., Patel P., Hawke T. J., Ceddia R. B. (2010) Dysregulation of lipolysis and lipid metabolism in visceral and subcutaneous adipocytes by high-fat diet: